

# Spatiotemporal distribution and speciation of silver nanoparticles in the healing wound

Marco Roman<sup>1\*</sup>, Chiara Rigo<sup>1</sup>, Hiram Castillo-Michel<sup>2</sup>, Dagmar S. Urgast<sup>3</sup>, Jörg Feldmann<sup>3</sup>, Ivan Munivrana<sup>4</sup>, Vincenzo Vindigni<sup>4</sup>, Ivan Mičetić<sup>5</sup>, Federico Benetti<sup>6</sup>, Carlo Barbante<sup>1,7</sup>, Warren R.L. Cairns<sup>7</sup>

<sup>1</sup> Ca' Foscari University of Venice, Department of Environmental Sciences, Informatics and Statistics (DAIS), Via Torino 155, 30172 Venice Mestre, Italy

<sup>2</sup> European Synchrotron Radiation Facility (ESRF), 71 avenue des Martyrs, 38000 Grenoble, France

<sup>3</sup> University of Aberdeen, Trace Element Speciation Laboratory, Aberdeen AB24 3UE, Scotland UK

<sup>4</sup> University Hospital of Padua, Burns Centre, Division of Plastic Surgery, Via Giustiniani 2, 35128 Padua, Italy

<sup>5</sup> University of Padua, Department of Biomedical Sciences, Via Ugo Bassi, 58/B35131 Padua, Italy

<sup>6</sup> EcamRicert Srl, European Centre for the Sustainable Impact of Nanotechnology (ECSIN), Corso Stati Uniti, 4 35127 Padua, Italy

<sup>7</sup> Institute for Polar Sciences (ISP-CNR), Via Torino 155, 30172 Venice Mestre, Italy

## \* Corresponding Author:

Marco Roman

Ca' Foscari University of Venice, Department of Environmental Sciences, Informatics and Statistics (DAIS), Via Torino 155, 30172 Venice Mestre, Italy

Phone: +0039 041 234 7731

E-mail: marco.roman@unive.it

## Supplementary information

### List of the acronyms

Ag	silver
BSA	bovine serum albumin
DLS	dynamic light scattering
ELS	electrophoretic light scattering
ESRF	European Synchrotron Radiation Facility
GSH	glutathione
HSS	human serum substitute
LA-ICP-MS	laser ablation-inductively coupled plasma-mass spectrometry
LCF	linear combination fitting
MALDI-TOF-MS	matrix-assisted laser desorption time-of-flight mass spectrometry
NPs	nanoparticles
SEM	scanning electron microscopy
SR- $\mu$ XANES	synchrotron radiation X-ray absorption near edge structure
TEM	transmission electron microscopy

TMAH	tetramethylammonium hydroxide
SR- $\mu$ XRF	synchrotron radiation micro x-ray fluorescence

## Experimental

### Standards and reagents

An Ag ICP-MS grade 1000  $\mu\text{g mL}^{-1}$  standard solution (certified, NIST traceable) was obtained from Ultra Scientific (Bologna, Italy) and was used to calibrate the total Ag measurements. Reference standards of metallic AgNPs of 10 nm nominal size, as citrate-stabilized water suspensions, were purchased from Sigma-Aldrich (Milan, Italy) and characterized as reported previously,<sup>1</sup> resulting to be  $9.2 \pm 3.2$  nm in size (average  $\pm \sigma$ , transmission electron microscopy -TEM-), spherical shape (TEM), good stability ( $\zeta$ -potential  $-46.4 \pm 2.2$  mV), and with a concentration of  $20.0 \pm 0.5$   $\mu\text{g mL}^{-1}$  as Ag (average  $\pm \sigma$ , ICP-MS). The commercial dressing Acticoat Flex3™ (Smith & Nephew, Milan, Italy) was used for *in vivo* treatment of burn patients following the general protocol reported elsewhere.<sup>2</sup>

Solid-state reference compounds used for SR- $\mu$ XANES speciation analysis included: metallic Ag foil, AgCl, Ag<sub>2</sub>SO<sub>4</sub>, AgNO<sub>3</sub>, Ag<sub>2</sub>O, Ag sulfadiazine (all from Sigma-Aldrich, Milan, Italy) and a fragment of intact Acticoat Flex3™ dressing. Reference standards of the AgNPs were prepared from the mother suspension by deposition of a 20  $\mu\text{L}$  drop between Ultralene® windows (Exacta+Optech Labcenter, Modena, Italy) and microscopy slides, followed by rapid freezing and freeze-drying for 24h. A standard of Ag bonded to glutathione (GSH) was prepared by incubating ionic Ag (from AgNO<sub>3</sub>, 10  $\mu\text{g mL}^{-1}$  as Ag) in an aqueous solution of reduced L-glutathione (Sigma-Aldrich, Milan, Italy) with a concentration of  $\sim 0.5$   $\text{mg mL}^{-1}$ , at 37 °C under gentle shaking for 2 h and in dark conditions, followed by freeze-drying as reported above.

Tetramethylammonium hydroxide (TMAH) 25% wt. in aqueous solution, Triton™ X-100 and NH<sub>4</sub>OH 25% wt. in aqueous solution were all purchased from Sigma-Aldrich; acetonitrile was purchased from Romil (Cambridge, UK).

### Characterization of the dressing and release of Ag *in vitro*

Extensive physico-chemical characterization of Acticoat Flex3™ and *in vitro* release experiments of Ag and AgNPs from the product have been carried out in previous works.<sup>1-4</sup> In this study, a few additional analyses were performed to provide further support to the overall interpretation of the observations carried out *in vivo*. The analyses included the determination of the pH-dependent colloidal stability and size distribution of primary NPs release in water, and the identification of Ag-binding proteins in a synthetic serum substitute as the release medium.

For colloidal stability and size distribution,  $\sim 130$  mg of the intact dressing were placed into 6 mL of ultrapure water at pH adjusted to 5, 6 and 7 (using NaOH), and then sonicated for 16 min at 37% amplitude in an ice bath using a Q700 (Qsonica, Newtown, CT, USA) device equipped with microtip probe. The suspension was centrifuged at 120 g for 10 min to settle major debris, and the supernatant was analyzed to determine the  $\zeta$ -potential by electrophoretic light scattering (ELS), and the size distribution by dynamic light scattering (DLS), using a Zetasizer Nano ZS system (Malvern Panalytical, Malvern, UK).

For the identification of Ag-binding proteins in human serum substitute (HSS, from Steamcell Technologies, Vancouver, Canada), release experiments were carried out as reported previously.<sup>1</sup> An aliquot (0.5 mL) of HSS after 72h of incubation with the dressing was transferred into a 3kDa cut-off membrane filter (Microcon Merck Millipore, Milan, Italy), centrifuged three times at 20000 g for 10 min (Eppendorf Microcentrifuge 5424, Milan, Italy) with double washing with ultrapure water to remove non-protein species, resulting in a ~4 fold preconcentration. Five  $\mu$ L of the solution recovered from the filter were diluted 100-fold in trifluoroacetic acid 0.1% vol. solution (in H<sub>2</sub>O/acetonitrile 1:1 vol.) and 1  $\mu$ L of the mix was deposited onto the appropriate stainless-steel sample holder and let dry. Analysis by MALDI-TOF-MS was performed using an instrument Ultraflex II (Bruker Daltonics, Bremen, Germany) with pulsed UV laser beam (nitrogen laser, 337 nm) and operating in linear positive ion mode. The instrumental parameters were the following: ion source voltage 1:25 kV; ion source voltage 2: 22.20 kV; delay time: 210 ns. External mass calibration was performed using the Protein Calibration Standard II (Bruker Daltonics), based on the average values of [M+H]<sup>+</sup> of trypsinogen, protein A, bovine serum albumin (BSA) and the average values of [M+2H]<sup>2+</sup> of protein A and BSA at m/z 23892, 44413, 66432, 22307 and 33216, respectively.

#### Patient recruitment

The study was carried upon approval by the Ethics Committee for Clinical Practice of the University Hospital of Padua (Prot. 28289/2016), and in accordance with the Declaration of Helsinki ethical guidelines, practice guidelines, and local laws and regulations. Informed written consent was obtained from all participants. Collection and storage of personal data was entirely managed by the medical doctors of the Burns Centre, who were responsible for patient care and collected the samples; sensitive data were stored in an IT system with limited access and were transmitted in a form that ensured anonymity. No financial support was provided to the patients.

The study involved four patients (A-D) providing skin samples through the bio-bank of the University Hospital of Padua. Patients were eligible for the study if affected by partial or full-thickness burns or equivalent wounds, while exclusion criteria were: i) known hypersensitivity to Ag and its compounds; ii) compromised immune system; any other pathology (diabetes; heart, renal and other disorders) or multiple traumas; iii) chemical or electrical burns; iv) being under 5 years or over 65 years of age. All patients were treated at the Burns Centre of the Hospital, by using the AgNP-containing dressing Acticoat Flex3<sup>TM</sup> as reported elsewhere,<sup>2</sup> and following current protocols without any additional invasive procedure.

Beside the general eligibility criteria reported above, patients were selected so to be representative of the distinct protocols used for wound treatment, and different healing progressions. In all cases, biopsy samples were collected from the wound bed before the first application of the dressing, and during treatment at consecutive time steps.

Patient A (male, age 63) had partial thickness bilateral burn on the legs and hands, due to backfiring in an open environment. Biopsies were performed on deep partial thickness wound regions of the right leg. The first sample was collected after surgical cleaning of the wound and before a single application of the dressing, which was kept on site after complete healing. Further biopsies were

performed at 3, 6, 9 and 12 days of treatment, corresponding to complete healing, from regions of interests at the wound margins above the dressing.

Patient B (male, age 54) was affected by a degloving injury of the left leg, equivalent to a full thickness burn lesion. The first sample was collected after surgical cleaning of the wound and before application of the dressing. At 4, 7 and 10 days of treatment (complete healing) the dressing was changed, and biopsies were performed contextually.

Patient C (female, age 56) had a full thickness flame burn to the thorax. The first sample was collected from the left axilla after surgical cleaning and before application of the dressing. Two additional biopsies were performed on the same area after 7 and 15 days of treatment in correspondence with dressing changes. At last sampling time, wound healing was still incomplete.

Patient D (male, age 48) had a partial thickness flame burn to both legs and arrived in the Burns Centre after emergency treatment with Ag sulfadiazine 1% cream in another hospital. The first biopsy was performed on the medial region of the right leg, after application of the cream and before surgical cleaning, and a second biopsy after 5 days of treatment with a single application of the dressing, when skin regeneration was still incomplete.

#### Biopsy samples collection and preparation

Full-thickness biopsy samples of the wounds were collected using a surgical punch of 4 mm i.d. and 7 mm of length. The samples were stored in plastic vials, immediately frozen at -80 °C without any preserving or fixing agent to maintain the distribution and speciation of Ag, they were then stored at -20 °C. No significant artifacts due to the growth of ice crystals were observed in the histological analysis of the tissues. Based on preliminary screening, specific patients and samples were selected to be dedicated to semi-quantitative imaging or speciation analysis with optimized respective preparation procedures, in order to maximize the probability to extract useful and representative results. Particularly SR- $\mu$ XANES analysis amongst the others requires a relatively high concentration of Ag for detection and reliable identification of Ag species, thus selection was based accordingly. For LA-ICP-MS analysis, the samples were cryosectioned longitudinally into 20  $\mu$ m thick slices, ensuring that the cutting direction remained perpendicular to the depth axis to avoid smearing of Ag along the profile. Notably, possible vertical smearing effects from punch sampling must be considered when evaluating the distribution of Ag at the section's margins. The sections were deposited onto uncoated microscope glass slides and were dried at room temperature overnight. The residual unsliced portion of the samples from patient B was used for quantitative Ag determination by bulk ICP-MS analysis. For SR- $\mu$ XRF and SR- $\mu$ XANES analyses, the samples were immediately frozen and stored at -80 °C until cryosectioning into slices of 30  $\mu$ m of thickness, placed between Ultralene covered microscopy slides, and freeze-drying overnight. Histological images were obtained for slices (thickness 20  $\mu$ m, ethanol stain followed by toluidine blue stain) adjacent to those that were analysed for elemental mapping and speciation.

#### Synchrotron radiation $\mu$ XRF and $\mu$ XANES analysis

High-resolution imaging of Ag distribution and single-point speciation of the metal in the skin profiles of patient A were determined by SR- $\mu$ XRF and Ag L<sub>III</sub>-edge SR- $\mu$ XANES analyses, respectively. The

measurements were performed using the scanning X-ray microscope of beamline ID21, at the European Synchrotron Radiation Facility (ESRF, Grenoble, France), operating in a vacuum at room temperature. Details on the instrumental parameters are provided elsewhere.<sup>1</sup> Energy selection was done by means of a double crystal (Si111) monochromator and detectors included a photodiode for  $I_0$  and an 80 mm active area Silicon Drift Detector (Bruker) for the emitted fluorescence. Focusing was achieved using fixed curvature Kirkpatrick-Baez mirror optics.

Small SR- $\mu$ XRF maps of Ag distribution were acquired for a preliminary analysis to select optimal regions for a full-profile scanning. The latter took from 8 to 12 h of time for acquisition, depending on the sample size.

Whole-profile SR- $\mu$ XRF imaging of Ag was performed in fluorescence mode with 3.42 keV of excitation energy, with a step (pixel) size of 2  $\mu\text{m}$  and integration time of 100 ms, whereas localized maps of regions of interest were obtained at 3 to 0.5  $\mu\text{m}$  pixel size. Other elements including P, S and Cl were also determined in all analyses to obtain structural information on the specimens. The raw data (counts) were elaborated using the software PyMca 4.7 (ESRF) as reported elsewhere<sup>1</sup> with some modifications. Briefly, the main steps of data elaboration were: i) correction for dead time and conversion of intensity data to counts per second (cps); ii) deconvolution (batch fitting of the SR- $\mu$ XRF spectra); iii) normalization for the incident beam flux; iv) subtraction of the background signal. The background signal was extracted from the whole-profile map of the sample collected from patient A before application of the dressing. The background intensity (68 cps) was calculated as the 99<sup>th</sup> percentile of the intensity distribution within an area of  $\sim 50,000$  pixels acquired with the same lateral resolution and integration time as the other maps. Single element or ternary plots were extracted without recurring to graphical interpolation.

The SR- $\mu$ XRF maps also provided a reference for spot selection of points of interest to collect Ag  $L_{III}$ -edge SR- $\mu$ XANES spectra in the 3.32 to 3.42 keV energy range with 0.5 eV steps. At least 10 spectra of 30 s were averaged for each spot, slightly changing the beam position from one spectrum to the next to avoid changes in speciation due to radiation damage. The spectra were elaborated and finally treated by linear combination fitting (LCF) using the software Athena 0.9.24 as reported elsewhere,<sup>1</sup> using the standards of pure Ag species reported above as input variables.

#### Laser ablation ICP-MS analysis

The semi-quantitative distribution of Ag in the skin profiles of patients B-D was determined by LA-ICP-MS imaging analysis. The samples from patient B were analysed at the University of Aberdeen using a New Wave 213 UP system (Fremont, CA, USA) equipped with a standard cell and coupled to an ICP-MS model 7500c from Agilent Technologies (Tokyo, Japan). The samples from patients C and D were analysed at Ca' Foscari University of Venice using a LSX-213 G2<sup>+</sup> system (Teledyne CETAC Technologies, Omaha, Nebraska, USA), equipped with a solid-state laser based on a YAG crystal doped with Nd ( $\text{Nd:Y}_3\text{Al}_5\text{O}_{12}$ ) and a HelEx<sup>TM</sup> two-volume cell, coupled to an ICP-MS model 7500cx from Agilent Technologies (Tokyo, Japan). The main instrumental parameters are reported in Supplementary Table S2. All analyses were carried out in scan line mode. Scan rate and laser energy were optimized for a complete ablation of the tissue without ablating the glass slide under the sample, while the laser spot size and space between lines were selected both within the range 6-50  $\mu\text{m}$  depending on the

resolution and the size of the scanned area of interest. The resulting lateral resolution ranged between 4 and 24  $\mu\text{m}$ , and the vertical resolution between 12 and 100  $\mu\text{m}$ . Connection to the ICP-MS was achieved using Tygon<sup>®</sup> tubing.

The ICP-MS lens voltages and gas flows were tuned daily for best sensitivity and stability (relative standard deviation < 5%) of the signal using the NIST612 certified reference material (trace elements in glass, National Institute of Standards and Technology, Gaithersburg, MD, USA) and monitoring the m/z 7, 89, 139, 175, and 208. The oxides were maintained below 1% with reference to the ratio  $^{232}\text{Th}^{16}\text{O}^+ / ^{232}\text{Th}^+$ . The ratio  $^{232}\text{Th}^+ / ^{238}\text{U}^+$  was kept close to one to minimize the effects of elemental fractionation during ablation. Silver was measured by monitoring both m/z 107 and 109 (as an internal consistency check), but final elaborations were based on the former mass. Carbon (m/z 13) and P (m/z 31) were also measured in all analyses to get structural information on the specimens, while Zn (m/z 67) was measured to investigate possible interactions with Ag dynamics. Background signals were acquired for 10 s before starting each ablation line and were subtracted from the sample intensities. The intensity data were converted into counts per second (cps), then all the scanned lines were pooled in a .dat file to be imported into the software PyMca to generate red-green-blue (RGB) plots without recurring to data interpolation, finally the tonality was eventually changed using the software Gimp 2.6.

The high-resolution semi-quantitative concentration profiles for patient B were calculated assuming that the mass-weighted average concentration of the low-resolution profiles, obtained by analysing one half of each sample, was representative of (coincided with) the total concentration in the corresponding slice analysed by LA-ICP-MS. For each map, the data points with a signal <100 cps (non-significant) were first removed. The distribution statistics (quartiles and maximum value) of signal intensity were calculated using all the aligned points for each depth increment. The average median along the whole profile was calculated and represented against the corresponding known bulk concentration of Ag to obtain a calibration curve (Supplementary Fig. S7), this was then used to convert the distribution statistics of signal intensity into a mass concentration. Statistica 10 (Statsoft) and Office Excel 365 (Microsoft Corporation) were used for data elaboration and graphical works.

The low-resolution quantitative determination of the Ag content in the same samples collected from patient B was performed as reported elsewhere.<sup>2</sup> Briefly, the specimens were cut manually using a scalpel, digested overnight in an alkaline TMAH solution at 60 °C, diluted in Triton X-100 0.1% vol. and  $\text{NH}_4\text{OH}$  2.8 % vol. aqueous solutions, and analysed using the Agilent 7500cx ICP-MS.

#### Comparison of SR $\mu$ XRF and LA-ICP-MS for bioimaging of Ag

Both LA-ICP-MS and SR- $\mu$ XRF techniques enable two-dimensional imaging of multi-elemental concentrations in solid samples over large scan areas (in the mm range) and within a reasonable time of analysis (8-12 h). In this study, their performances were comparable in terms of sensitivity for Ag, estimated at  $\sim 200$  cps  $\mu\text{m}^{-2}$  per  $\text{pg mg}^{-1}$  of the metal for the present samples (slices of 25  $\mu\text{m}$  thickness,

0.1 s integrations time). While SR- $\mu$ XRF has a fixed high spatial resolution (beam size  $\sim 1 \mu\text{m}$ ), in LA-ICP-MS the beam size is tunable (from 5 to 200  $\mu\text{m}$  with the instrument used in this study), meaning that in case of low concentrations, the absolute signal intensity can be improved by decreasing spatial resolution. Indeed, given the comparable sensitivity reported above, with a beam size of 1  $\mu\text{m}$  and 50  $\mu\text{m}$  for  $\mu$ XRF and LA-ICP-MS respectively, the estimated respective limits of detection (LODs) for Ag were  $60 \text{ ng mg}^{-1}$  and  $0.25 \text{ ng mg}^{-1}$ . Laser ablation -ICP-MS allows the measurement of other elements such as Zn, which could not be measured simultaneously with the Ag L-alpha line using SR- $\mu$ XRF (Zn K alpha requires an excitation energy  $>10 \text{ keV}$ , while an efficient and sensitive detection of Ag requires working at 3.5 keV). These features make LA-ICP-MS an ideal technique to gain semi-quantitative information about the concentrations of Ag and its spatial variability within large sample regions. However, since LA-ICP-MS is a destructive technique with limited precision for soft non-embedded materials, it is less reliable when comparing the elemental distributions and structural characteristics of the biological tissue at the micrometric scale. For this issue SR- $\mu$ XRF is better suited, being non-destructive and capable of reaching a higher spatial resolution. In addition, this technique allows us to point at specific regions of interest based on the resulting elemental maps, and to perform high resolution single-point speciation analysis by SR- $\mu$ XANES. Speciation imaging is also possible, as recently explored in a complementary work.<sup>1</sup>

## References

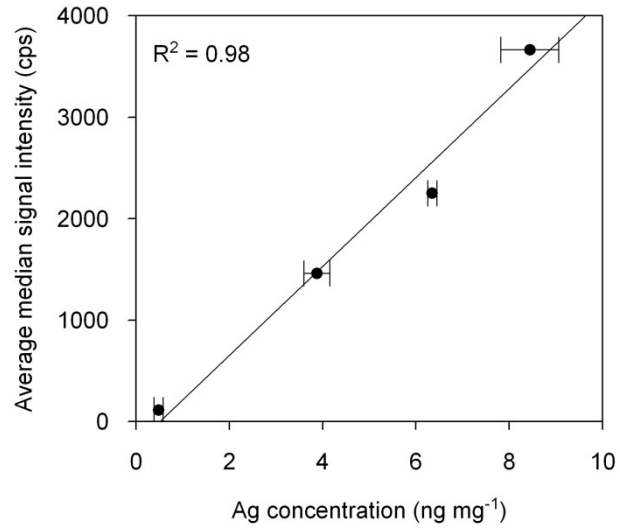
- 1 M. Roman, C. Rigo, H. Castillo-Michel, I. Munivrana, V. Vindigni, I. Mičetić, F. Benetti, L. Manodori and W. R. L. Cairns, *Anal. Bioanal. Chem.*, 2016, **408**, 5109–5124.
- 2 C. Rigo, L. Ferroni, I. Tocco, M. Roman, I. Munivrana, C. Gardin, W. R. L. Cairns, V. Vindigni, B. Azzena, C. Barbante and B. Zavan, *Int. J. Mol. Sci.*, 2013, **14**, 4817–40.
- 3 C. Rigo, M. Roman, I. Munivrana, V. Vindigni, B. Azzena, C. Barbante and W. R. L. Cairns, *Burns*, 2012, **38**, 1131–1142.
- 4 M. Roman, C. Rigo, I. Munivrana, V. Vindigni, B. Azzena, C. Barbante, F. Fenzi, P. Guerriero and W. R. L. Cairns, *Talanta*, 2013, **115**, 94–103.

**Supplementary Table S1.** Semi-quantitative speciation of Ag in the scar and wound of patient A obtained by linear combination fitting (LCF) of the SR- $\mu$ XANES spectra.

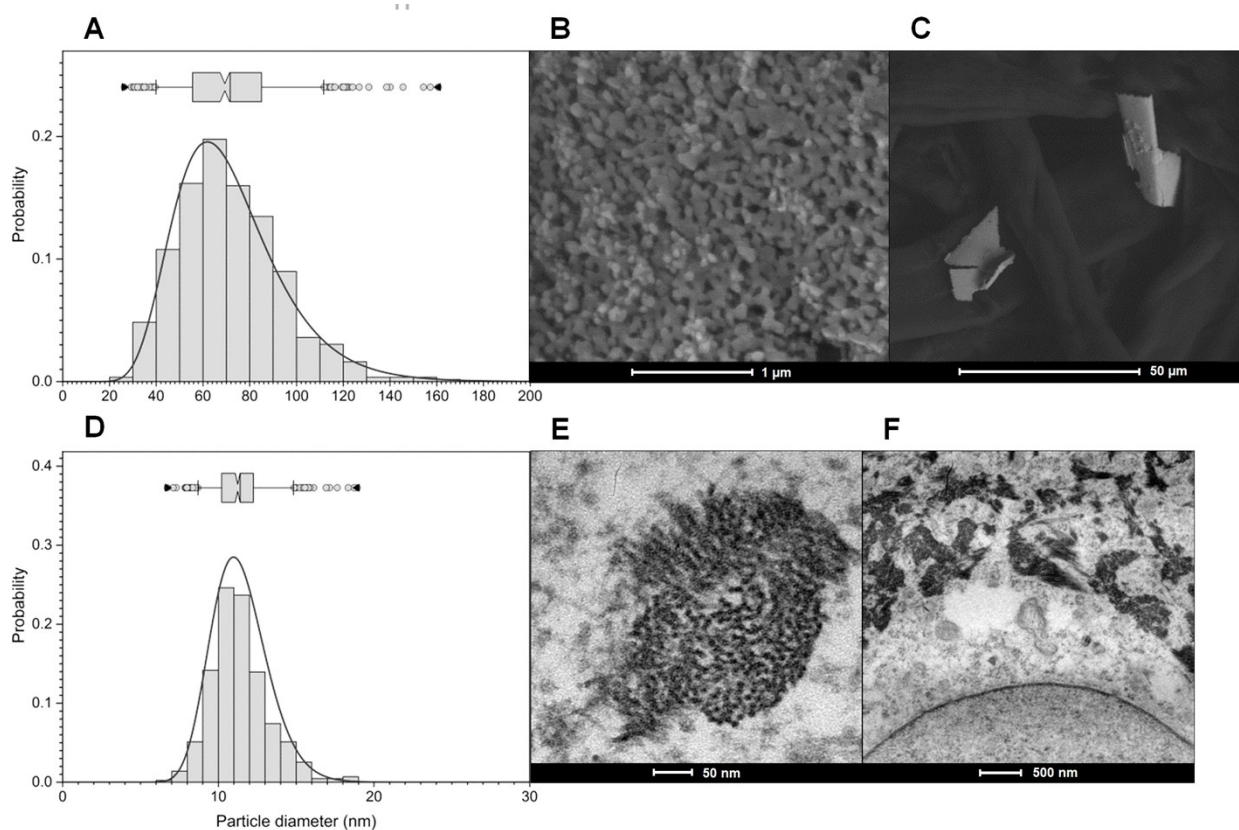
Sample/Spectrum	Fitting variables	Molar fraction %	NSS %
6 days spot 1	AgCl	59(4)	0.026(0.007)
	Ag <sup>0</sup> NPs 10 nm	31(2)	
	other	10(2)	
6 days spot 2	AgCl	56(5)	0.024(0.001)
	Ag <sup>0</sup> NPs 10 nm	35(2)	
	other	9(3)	
6 days spot 3	AgCl	73	0.004
	Ag <sup>0</sup> NPs 10 nm	16	
	AgGSH	11	
6 days spot 4	AgCl	55	0.012
	AgGSH	45	
6 days spot 5	AgGSH	68	0.012
	AgCl	32	
6 days spot 6	AgCl	48	0.045
	Ag <sup>0</sup> NPs 10 nm	23	
	other	29	
3 days spot	AgGSH	81	0.025
	other	19	

**Supplementary Table S2.** Instrumental parameters adopted for LA-ICP-MS analysis.

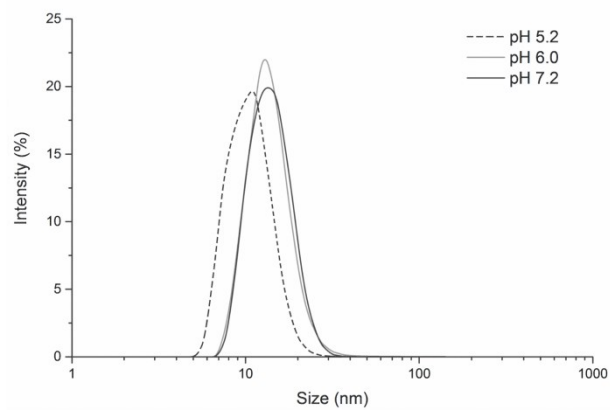
<b>Patient-Figure</b>	<b>B-4A</b>	<b>B-4B</b>	<b>C-5, D-S4</b>
<b>LA parameters</b>			
Instrument	New Wave 213 UP	New Wave 213 UP	Cetac LSX 213G2 <sup>+</sup>
Sampling area diameter ( $\mu\text{m}$ )	50	6	20
Space between lines ( $\mu\text{m}$ )	50	6	8
Scan speed ( $\mu\text{m s}^{-1}$ )	50	5	22.8
Frequency (Hz)	10	10	10
Energy (%)	35	45	10
Fluence ( $\text{J cm}^{-2}$ )	0.1	0.1	1
Fluxes He1, He2 ( $\text{mL min}^{-1}$ )			500, 300 $\text{mL min}^{-1}$
<b>ICP-MS parameters</b>			
Instrument	Agilent 7500c	Agilent 7500c	Agilent 7500cx
Acquired m/z (integration time, s)	13 (0.02); 31, 34 (0.05); 67 (0.15); 107, 109 (0.1)	13, 31, 34 (0.05 s); 67, 107, 109 (0.2 s)	13, 31, 34 (0.1 s); 67, 107, 109 (0.2 s)
RF power (W)	1360	1360	1350
Carrier gas ( $\text{mL min}^{-1}$ )	1.45	1.45	0.75



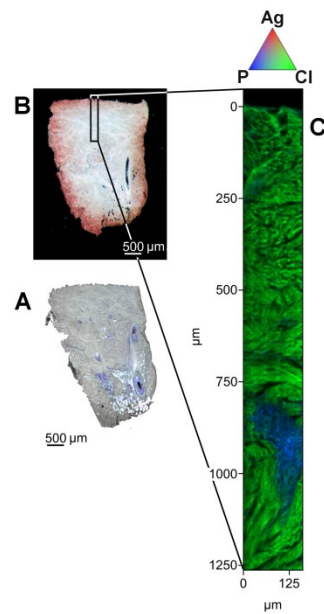
**Supplementary Figure S1.** Calibration curve of average median signal intensity (cps) vs. bulk mass concentration (ng mg<sup>-1</sup>, average $\pm\sigma$ ) of Ag for the LA-ICP-MS maps (patient B) used to extract high-resolution semi-quantitative concentration profiles.



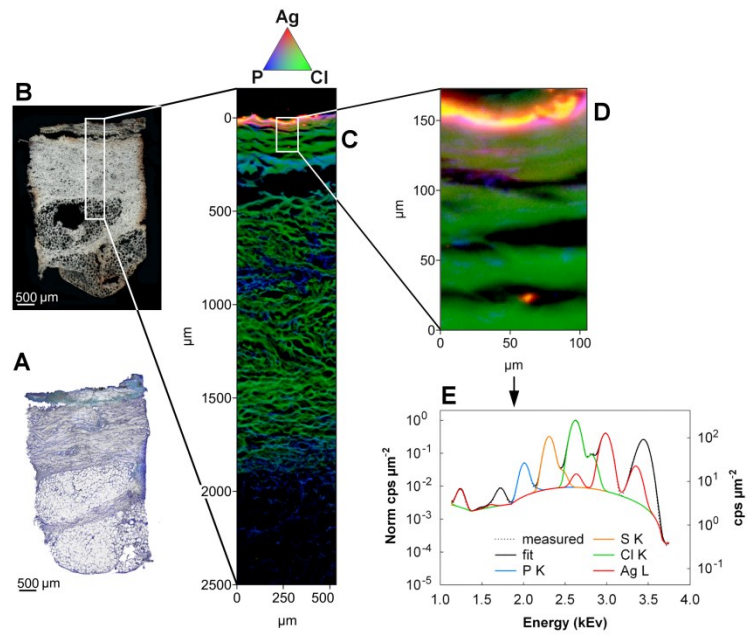
**Supplementary Figure S2.** (A) Size distribution of AgNPs on the surface (B) of coating agglomerates (C) detached from the AgNP-containing dressing after static incubation in human serum substitute (SEM analysis, results from a previous study,<sup>3</sup> unpublished images). (D) Size distribution of AgNPs agglomerates (E, F) detected in fibroblasts of a burn patient treated with the dressing (TEM analysis, results from a previous study,<sup>2</sup> unpublished data and images).



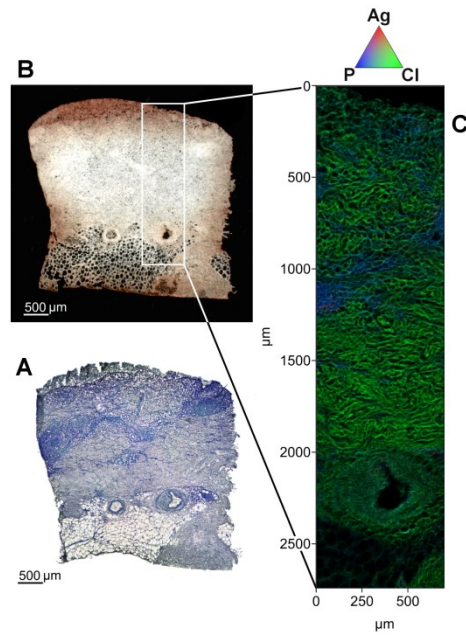
**Supplementary Figure S3.** Size distribution (hydrodynamic diameter) of particles released by sonication of the AgNPs-containing dressing in water as function of the pH, determined by DLS analysis.



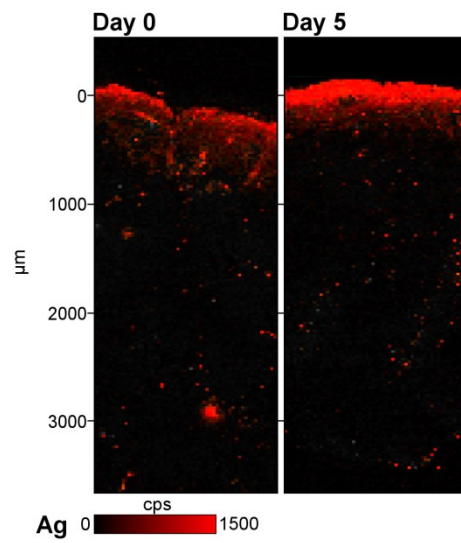
**Supplementary Figure S4.** Full profile biopsy of the wound of patient A before application of the AgNP-containing dressing, analysed by SR- $\mu$ XRF. (A) Histological image of the tissue (adjacent slice). (B) Picture of the analysed slice. The scanned area locates in the black frame. (C) Ternary RGB map of signal intensities (cps) of Ag (log scale, full scale 150 cps), P and Cl (linear scales, full scales 10000 and 30000 cps, respectively); pixel size 2  $\mu$ m.



**Supplementary Figure S5.** Full profile biopsy of the wound of patient A, six days after a single application of the AgNP-containing dressing, analysed by SR- $\mu$ XRF. (A) Histological image of the tissue (adjacent slice). (B) Picture of the analysed slice. The scanned area locates in the white frame. (C) Ternary RGB map of signal intensities (cps) of Ag (log scale, full scale 300000 cps), P and Cl (linear scales, full scales 15000 and 10000 cps, respectively); pixel size 2  $\mu$ m. (D) zoom RGB map of the region located in the frame (independent acquisition), same scales as in (C); pixel size 1  $\mu$ m. (E) Average SR- $\mu$ XRF spectrum of the whole zoom map area.



**Supplementary Figure S6.** Full profile biopsy of the wound of patient A, twelve days after a single application of the AgNP-containing dressing, analysed by SR- $\mu$ XRF. (A) Histological image of the tissue (adjacent slice). (B) Picture of the analysed slice. The scanned area locates in the white frame. (C) Ternary RGB map of signal intensities (cps) of Ag (log scale, full scale 500 cps), P and Cl (linear scales, full scales 10000 and 40000 cps, respectively); pixel size 2  $\mu$ m.



**Supplementary Figure S7.** Maps of Ag distribution in the skin profile from patient D, pre-treated with Ag sulfadiazine, before application of the AgNP-containing dressing (Day 0) and after 5 days (Day 5). Data obtained by LA-ICP-MS with pixel size 24 x 30  $\mu\text{m}$ ; signal intensity is expressed in cps with linear scale.